Eur J Nucl Med Mol Imaging (2007) 34:722–733
DOI 10.1007/s00259-006-0266-4

ORIGINAL ARTICLE

Imaging of HER2-expressing tumours using a synthetic Affibody molecule containing the ^{99m}Tc-chelating mercaptoacetyl-glycyl-glycyl-glycyl (MAG3) sequence

Torun Engfeldt · Anna Orlova · Thuy Tran · Alexander Bruskin · Charles Widström · Amelie Eriksson Karlström · Vladimir Tolmachev

Received: 4 March 2006 / Accepted: 10 August 2006 / Published online: 5 December 2006

Abstract
Purpose Expression of human epidermal growth factor receptor type 2 (HER2) in malignant tumours possesses well-documented prognostic and predictive value. Non-invasive imaging of expression can provide valuable diagnostic information, thereby influencing patient management. Previously, we reported a phage display selection of a small (about 7 kDa) protein, the Affibody molecule $Z_{HER2:342}$, which binds HER2 with subnanomolar affinity, and demonstrated the feasibility of targeting of HER2-expressing xenografts using radioiodinated $Z_{HER2:342}$. The goal of this study was to develop a method for ^{99m}Tc labelling of $Z_{HER2:342}$ using the MAG3 chelator, which was incorporated into $Z_{HER2:342}$ using peptide synthesis, and evaluate the targeting properties of the labelled conjugate.
Methods MAG3-$Z_{HER2:342}$ was assembled using Fmoc/tBu solid phase peptide synthesis. Biochemical characterisation of the agent was performed using RP-HPLC, ESI-MS, biosensor studies and circular dichroism. A procedure for ^{99m}Tc labelling in the presence of sodium/potassium tartrate was established. Tumour targeting was evaluated by biodistribution study and gamma camera imaging in xenograft-bearing mice. Biodistribution of ^{99m}Tc-MAG3-$Z_{HER2:342}$ and ^{125}I-*para*-iodobenzoate -$Z_{HER2:342}$ was compared 6 h p.i.
Results Synthetic MAG3-$Z_{HER2:342}$ possessed an affinity of 0.2 n*M* for HER2 receptors. The peptide was labelled with ^{99m}Tc with an efficiency of about 75–80%. Labelled ^{99m}Tc-MAG3-$Z_{HER2:342}$ retained capacity to bind specifically HER2-expressing SKOV-3 cells in vitro. ^{99m}Tc-MAG3-$Z_{HER2:342}$ showed specific tumour targeting with a contrast similar to a radioiodinated analogue in mice bearing LS174T xenografts. Gamma camera imaging demonstrated clear and specific visualisation of HER2 expression.
Conclusion Incorporation of a mercaptoacetyl-containing chelating sequence during chemical synthesis enabled site-specific ^{99m}Tc labelling of the $Z_{HER2:342}$ Affibody molecule with preserved targeting capacity.

Keywords HER2 · Technetium-99m · Targeting · Peptide · Biodistribution

T. Engfeldt · A. E. Karlström
School of Biotechnology, Division of Molecular Biotechnology,
Royal Institute of Technology,
Stockholm, Sweden

A. Orlova · T. Tran · A. Bruskin · V. Tolmachev (✉)
Biomedical Radiation Sciences, Rudbeck Laboratory,
Uppsala University,
Uppsala, Sweden
e-mail: Vladimir.Tolmachev@bms.uu.se

A. Orlova · V. Tolmachev
Affibody AB,
Bromma, Sweden

C. Widström
Department of Hospital Physics, Uppsala University Hospital,
Uppsala, Sweden

Introduction

Human epidermal growth factor receptor type 2 (HER2), also known in the literature as ErbB2 or p185, is a transmembrane tyrosine kinase receptor belonging to the human epidermal growth factor receptor family. HER2 signalling causes increased mitotic activity, increase of cell motility and suppression of apoptosis. Expression of HER2 has been detected in a number of malignant tumours, such as carcinomas of breast, ovary and urinary bladder, and is

considered to be part of the malignant phenotype [1–3]. Blocking of HER2 signalling in breast carcinomas using the monoclonal antibody trastuzumab (Herceptin®) results in an increase in survival and trastuzumab is approved for clinical use in both Europe and North America. Numerous studies report that HER2 expression in breast carcinomas is associated with tumour sensitivity to treatment with trastuzumab and anthracycline-based adjuvant therapy [4, 5]. There are also reports indicating that HER2 expression is associated with decreased overall survival, high probability of early tumour relapse and resistance to cyclophosphamide/methotrexate/fluorouracil (CMF) therapy [6–9].

Detection of HER2 expression in, for example, breast cancer provides important diagnostic information influencing patient management. Guidelines of The American Society of Clinical Oncology recommend evaluation of HER2 expression on every primary breast cancer either at the time of diagnosis or at the time of recurrence [10]. The use of radionuclide molecular imaging would enable detection of HER2 by a non-invasive procedure in both primary tumours and metastases, without false-negative results due to sampling errors. Clinical utility of radionuclide imaging of HER2 expression in breast cancer patients has been demonstrated by Behr and co-workers [11]. The use of ^{111}In-DTPA-trastuzumab made it possible to identify both patients responding to trastuzumab treatment and patients who may suffer from toxicity associated with such treatment.

Radionuclide targeting of HER2, for both imaging and therapy, using intact antibodies has already been evaluated [11–19]. However, slow tumour targeting and slow blood clearance of intact immunoglobulins are well-recognised problems, and down-sizing of targeting agents seems to be crucial in future nuclear medicine, at least for imaging [20, 21]. Experiments with different antibody fragments have demonstrated the possibility of obtaining high tumour-to-non-tumour ratios shortly after injection in the case of HER2 targeting [22–25].

One way to circumvent the limitations of using large antibodies is the use of smaller, alternative affinity proteins. Affibody molecules constitute one such class of binding molecules that originate from the 58 amino acid cysteine-free scaffold of the staphylococcal protein A-derived Z domain. The scaffold has been subjected to randomisation of 13 surface-exposed residues to generate a library from which high-affinity binders have been selected by phage display [26]. Affibody molecules have recently emerged as attractive alternatives to antibodies in a number of biotechnological applications such as affinity chromatography [27], ELISA [28], Western blots [29] and protein capture microarrays [30]. The Affibody molecule $Z_{HER2:4}$, which binds to HER2 with an affinity of 50 n*M*, was selected and demonstrated an ability to bind specifically to HER2-expressing cells after indirect radioiodination [31]. The dimeric form, $(Z_{HER2:4})_2$, with an affinity of 3 n*M* [32], has been used for HER2 targeting in a murine xenograft model, resulting in high tumour-to-non-tumour ratio within a few hours after injection when radioiodine [33] or radiobromine [34] labels were used. Affinity maturation of $Z_{HER2:4}$ provided a new clone, $Z_{HER2:342}$, which binds to HER2 with an apparent affinity of 22 p*M*. Radioiodinated $Z_{HER2:342}$ has demonstrated a clear advantage in tumour targeting over both dimeric and monomeric forms of the parental clone [35]. To make kit formulation possible and to improve the logistics of the clinical use, methods for ^{111}In-labelling of $Z_{HER2:342}$ using isothiocyanate derivatives of benzyl-DTPA [36, 37] and benzyl-DOTA (Orlova, unpublished results 2005-6) have been developed. Still, development of a ^{99m}Tc label for $Z_{HER2:342}$ is desirable owing to the excellent imaging properties, low price and straightforward logistics of this nuclide [38]. Previously, we evaluated the labelling of His_6-$(Z_{HER2:4})_2$ with ^{99m}Tc using Tc(I)-carbonyl chemistry [39]. The labelled conjugate was stable in vivo and demonstrated good targeting of HER2 expression in a murine xenograft model. However, ^{99m}Tc-His_6-$(Z_{HER2:4})_2$ showed high uptake in liver. High and persistent liver uptake was also detected when this method was applied to the affinity matured monomer His_6-$Z_{HER2:342}$ (Orlova, unpublished results 2005). It is recognised that the biodistribution of ^{99m}Tc-labelled peptides can be modified to a high extent by the use of an appropriate chelator [40, 41].

The aim of this study was to evaluate the chelating mercaptoacetyl-glycyl-glycyl-glycyl sequence (MAG3) as a linker for coupling of ^{99m}Tc to the anti-HER2 $Z_{HER2:342}$ Affibody molecule.

Previously, both pre-labelling and post-labelling of MAG3 with different protective groups have been utilised for labelling of antibodies [42] and their Fab [43] and dsFv fragments [44], peptides [40, 41, 45] and antisense DNA [46], demonstrating good in vivo stability. Both approaches, however, are usually based on the coupling of the chelator to the targeting macromolecule in solution, which typically results in a heterogeneous mixture of tracers with different numbers of chelators owing to multiple reactive groups in the peptides and proteins. The relatively small size enables a direct chemical peptide synthesis of Affibody molecules at high yield [47]. By using synthetic chemistry, the chelator can be introduced site specifically, thus generating homogeneous tracer with well-defined properties. This approach has been applied for synthesis of bombesin analogues containing MAG3 [48].

The goal of this study was to synthesise MAG3-$Z_{HER2:342}$ and evaluate the feasibility of its use for visualisation of HER2 expression in malignant tumours using ^{99m}Tc as a label.

Materials and methods

Materials

All Fmoc protected amino acids were purchased from Applied Biosystems (Foster City, CA, USA). *Tert*-butyl (tBu) was used as side chain protection group on Asp, Glu, Ser, and Tyr, *tert*-butyloxycarbonyl (Boc) – Lys and Trp, trityl (Trt) – Asn and Gln, 2,2,4,6,7-pentamethyldihydrobenzofuran-5-sulfonyl (Pbf) – Arg. 1-Hydroxybenzotriazole (HOBt) and 2-(1*H* -benzotriazol-1-yl)-1,1,3,3-tetramethyluronium hexafluorphosphate (HBTU) were from Advanced ChemTech (Louisville, KY, USA). *N*-Ethyldiisopropylamine (DIEA) and piperidine were from Lancaster Synthesis (Morecambe, UK). *S*-Trityl-mercaptoacetic acid (Trt-HSAc) was from AnaSpec Inc (San Jose, CA, USA). Triisopropylsilane (TIS), trifluoroacetic acid (TFA) and *tert*-butyl methyl ether were purchased from Merck. Acetic acid and *N*-methylpyrrolidone (NMP) were from VWR International (Stockholm, Sweden). Ethanedithiol (EDT) was from Aldrich (St.Louis, MO, USA). Acetic anhydride and dichloromethane (DCM) were from Applied Biosystems, (Warrington, UK). Dithiothreitol (DTT) and iodoacetamide were from Sigma (Steinheim, Germany). ^{99m}Tc was obtained as pertechnetate by elution of Ultra-TechneKow generator, Tyco, with sterile 0.9% sodium chloride (Mallinckrodt Medical BV, Petten, The Netherlands).

Radioactivity measurements

The radioactivity was measured using an automated gamma counter with a 3-inch NaI(Tl) detector (1480 WIZARD, Wallac Oy, Turku, Finland). The distribution of radioactivity along the instant thin-layer chromatography strips or PAGE gels was measured on the Cyclone Storage Phosphor System (Packard) and analysed using the OptiQuant image analysis software (OptiQuant). Cells were counted using an electronic cell counter (Beckman Coulter, Switzerland).

Peptide synthesis

Affibody molecule $Z_{HER2:342}$ was synthesised on a 433A Peptide Synthesizer (Applied Biosystems) using standard Fmoc chemistry, essentially as described in Engfeldt et al. [47]. The peptide $Z_{HER2:342}$ (VENKFNKEMRNAY WEIALLPNLNNQQKRAFIRSLYDDPSQSANL LAEAKKLNDAQAPK) was assembled on an Fmoc amide resin with a substitution level of 0.67 mmol/g. The N-terminal Fmoc group was removed by 20% piperidine-NMP. Acylation reactions were performed in NMP with 10 molar equivalents of amino acid, activated with HBTU and HOBt. The 17 underlined residues in the sequence above were double coupled. Unreacted amino groups were capped with acetic anhydride.

The Tc-chelating function MAG3 was introduced by manual synthesis. The N-terminal Fmoc protecting group was removed by incubation with 20% piperidine-NMP for 20 min. All manual acylation reactions were performed with 5 molar equivalents of amino acid, HBTU and HOBt and 10 equivalents of DIEA in NMP for 20 min. All reactions were monitored by the Kaiser test, and repeated when the yield was found to be unsatisfactory.

The final deprotection and release of peptides from the resin support was performed as a one-step procedure by treatment with TFA/EDT/TIS/H_2O (94:2.5:2.5:1) for 2 h, followed by three rounds of extraction in *tert*-butyl methyl ether-H_2O (50:50), filtration and lyophilisation. The product was analysed by analytical reversed phase high-performance liquid chromatography (RP-HPLC) using a 4.6×150 mm polystyrene/divinylbenzene matrix column with a particle size of 5 μm (Amersham Biosciences), a 20-min gradient of 20–60% B (A: 0.1% TFA-H_2O; B: 0.1% TFA-CH_3CN) and a flow rate of 1 ml/min. The peptides were purified using a 20-min gradient of 25–45% B. The pure product was lyophilised prior to dissolving in 10 m*M* NH_4Ac pH 5,5 and the final peptide concentration was determined by amino acid analysis (Aminosyraanalyscentralen, Uppsala, Sweden).

To verify the identity of the peptides, part of the fractions from the HPLC analysis were lyophilised, dissolved in 5 *M* urea, 0.2 *M* NH_4HCO_3 and 30 m*M* DTT and incubated for 1 h to reduce disulphides before capping free thiol groups with iodoacetamide (0.1 *M*, 1 h), and finally the peptide mass was analysed on a Q-Tof™ II mass spectrometer fitted with an ESI source (Waters Corporation, Micromass MS Technologies, Manchester, UK). The Maximum Entropy™ 1 (MaxEnt1) algorithm was used to deconvolute isotopic and charge state information.

Melting point analysis

Variable temperature measurements were performed using a JASCO J-810 spectropolarimeter (JASCO, Tokyo, Japan). Samples were diluted to a concentration of 50 μ*M* in PBS pH 7.4. A cell with an optical path length of 1 mm was used. CD spectra from 250 to 195 nm were obtained at 20°C before and after melting tests. For melting point measurements, the absorbance was measured at 221 nm and the temperature was increased by 5°C/min from 20° to 90°C.

Biosensor analysis

Real-time biospecific interaction analysis was used to study the binding kinetics of $Z_{HER2:342}$ and MAG3-$Z_{HER2:342}$ on a Biacore 2000 instrument (Biacore, Uppsala, Sweden).

Recombinant extracellular domain of HER2 (a generous gift from Prof. Gregory Adams, Fox Chase Cancer Center, Philadelphia) and the control protein human serum albumin, HSA (KabiVitrum, Stockholm, Sweden), were diluted to 20 μg/ml in 10 m*M* NaAc pH 4.5 and immobilised onto a CM5 sensor chip (Biacore). The immobilisation level was 500 RU (response units) for the HER2 surface and 900 RU for HSA. Samples were diluted in HBS (10 m*M* HEPES, 150 m*M* NaCl, 3.4 m*M* EDTA, 0.005% Surfactant P20, pH 7.4) to concentrations ranging from 0.3 to 10 n*M*. The flow rate was set to 50 μl/min with HBS as running buffer, and the samples were injected for 5 min followed by 10-min dissociation and regeneration with 20 μl HCl (20 m*M*). The BiaEval software (Biacore) and the Langmuir 1:1 binding model were used for the kinetic analysis.

Labelling with ^{99m}Tc and stability tests

Before labelling, freeze-dried MAG3-$Z_{HER2:342}$ was dissolved in degassed Milli-Q water and stored at −20°C. Analysis of the labelled Affibody molecules was performed using glass fibre sheets impregnated with silica gel for instant thin-layer chromatography (ITLC SG, Gelman Sciences Inc). To determine labelling yield and stability, ITLC SG strips were eluted with PBS. Validation experiments demonstrated that pertechnetate, as well as tartrate, glucoheptonate and cysteine complexes of ^{99m}Tc migrate with the eluent front, while Affibody molecules do not move under these conditions. To determine the presence of reduced hydrolysed technetium, ITLC was eluted with pyridine:acetic acid:water (5:3:1.5). When this eluent was used, the technetium colloids stayed, while radiolabelled Affibody molecules as well as pertechnetate and tartrate complexes of ^{99m}Tc migrated with the solvent front.

The labelling method was similar to that described by Winnard et al. [49]. Aqueous solution 20 μl MAG3-$Z_{HER2:342}$ (1 mg/ml) was mixed with 80 μl PBS, 20 μl of a solution containing Na/K tartrate in 0.5 *M* $NaHCO_3$ and 0.25 *M* NH_4OAc, and solution of $SnCl_2 \cdot H_2O$ in 0.01 *M* HCl (10 μl, 1 mg/ml) was added. To this mixture, 50–350 μl of fresh Tc-generator eluate was added and the mixture was incubated at room temperature for 60 min.

After labelling, ^{99m}Tc-MAG3-$Z_{HER2:342}$ was isolated from unreacted technetium and other low molecular weight components using size-exclusion chromatography with a disposable NAP-5 column (Amersham Pharmacia Biotech) pre-equilibrated with PBS. Separation was performed according to the manufacturer's instructions.

Stability tests were performed when labelled Affibody molecules were incubated in PBS or in PBS with 300 molar equivalents of cysteine. Stability was analysed by ITLC.

To analyse serum stability, blood was collected from ten NMRI mice using heparinised syringe. The blood was centrifuged at 5,000 *g*, and serum was collected, divided into 0.5-ml aliquots and stored frozen before use. Serum samples were thawed immediately before the stability test. The serum stability test was performed in triplicate. Serum samples (240 μl) were mixed with freshly labelled ^{99m}Tc-MAG3-$Z_{HER2:342}$ (10 μl) to obtain an Affibody molecule concentration similar to the concentration in blood at the time of injection. Samples were incubated at 37°C for 1 h. After incubation, tested samples were analysed by SDS PAGE on NuPAGE 4–12% Bis-Tris Gel (Invitogen) in MES buffer (200 V constant). To facilitate interpretation of the results, a sample of ^{99m}Tc-pertechnetate, and a sample of ^{99m}Tc-MAG3-$Z_{HER2:342}$, which was not treated in blood serum, were run in parallel with the test sample on the same gel. After analysis, gels were dried, and radioactivity distribution along gels was evaluated using a Cyclone Storage Phosphor System (Packard).

Cell cultures

SKOV-3 (1.2×10^6 HER2 receptors per cell [19]) cells, which were used in the in vitro experiments, were cultivated on Petri dishes with a diameter of 3.5 cm to a cell density of $2–5 \times 10^5$ cells per dish. The LS174T cell line was used in the in vivo experiments. According to Milenic and co-authors [50, 51], this cell line possesses low but uniform expression of HER2 and may be a good model to demonstrate the sensitivity of ^{99m}Tc-MAG3-$Z_{HER2:342}$ in the detection of low-level antigen expression.

Binding specificity of ^{99m}Tc-labelled MAG3-$Z_{HER2:342}$ to HER2-expressing SKOV-3 cells

Labelled conjugates, 0.8 ng/10^5 cells, were added to two groups of Petri dishes containing SKOV-3 cells. One group of dishes was pre-saturated with a 1,000-fold excess of unlabelled recombinant Affibody molecules $Z_{HER2:342}$ 10 min before the labelled Affibody molecules were added. The cells were incubated for 1 h at 37°C and incubation media was collected. The cell dishes were washed with cold serum-free medium and treated with 0.5 ml trypsin-EDTA solution (0.25% trypsin, 0.02% EDTA in PBS buffer, Flow Irvine, UK) for 10 min at 37°C. When cells were detached, 0.5 ml complete medium was added to every dish and cells were re-suspended. The cell suspension was collected for radioactivity measurements. Cell-associated radioactivity (*C*) was measured on an automated gamma counter in parallel with 1 ml corresponding incubation medium (*M*). The fraction of added radioactivity bound to cells was calculated as % of bound radioactivity = $C \times 100\%/(C+M)$.

In order to facilitate interpretation of the results of the cellular studies, we attempted to determine the internalised fraction by acid wash, similar to a method earlier applied to

EGF-based conjugates [52]. However, validation experiments showed that this method could not remove the radioactivity completely from the cell surface after incubation on ice, probably owing to the very strong binding of radiolabelled $Z_{HER2:342}$ to HER2 (data not shown). This means that acid wash would overestimate internalised radioactivity. For this reason, quantitative internalisation assay was not performed.

Cellular retention after interrupted incubation with ^{99m}Tc-MAG3-$Z_{HER2:342}$

Labelled conjugate, 0.8 ng/10^5 cells, was added in 1 ml complete medium to a series of Petri dishes containing SKOV-3 cells. The dishes were incubated for 2 h at 37°C and the incubation medium was removed. The cells were washed six times with ice-cold serum-free medium, and after addition of 1 ml complete medium the cell dishes were incubated further at 37°C. At designed times of incubation (0.5, 1, 1.5, 2, 4, 6, 8 and 24 h), one group of three dishes was analysed for cell-associated radioactivity. Medium was collected in scintillation tubes; cells were washed six times with ice-cold serum-free medium and treated with 0.5 ml trypsin-EDTA solution for 10 min at 37°C. After addition of 0.5 ml complete medium, the cells were re-suspended and collected in scintillation tubes. The radioactivity content of the samples was measured by an automated gamma counter.

Antigen binding capacity

The SKOV-3 cells were scraped from the surface in order to preserve the receptor expression. After re-suspension of scraped cells in medium, they were counted in an automated cell counter and cell pellets containing 6×10^6 cells were formed in Eppendorff tubes by gentle centrifugation (2,500 *g*). The analysis was made in triplicate. The supernatant was removed completely and 1 ml of medium with labelled conjugate (ratio of approximately 1 Affibody molecule per 100 HER2 receptors) was added. The cells were gently re-suspended and incubated for 4 h at 4°C under slight shaking. After incubation, the cells were centrifuged (7,500 *g*) and 0.5 ml supernatant medium was taken to the separate Eppendorff tube. The radioactivity was measured on both samples and the antigen binding capacity (ABC) was calculated as $\mathrm{ABC} = (A - B)/(A + B) \times 100\%$, where A is the radioactivity of the Eppendorff tube containing both cell pellet and 0.5 ml supernatant, and B is the radioactivity of the Eppendorff tube containing 0.5 ml supernatant only.

Animal tumour model

The animal study was approved by the local Ethics Committee for Animal Research. Female outbreed Balb/c *nu*/*nu* mice (10–12 weeks old at arrival) were used in the in vivo experiments. The LS174T tumours were grafted by subcutaneous (s.c.) injection of ~10^6 cells in the right hind leg. Xenografts were allowed to develop during a period of 2 weeks. The SKOV-3 tumours were grafted by s.c. injection of ~7×10^6 cells in the right hind leg. Xenografts were allowed to develop during a period of 8 weeks.

Biodistribution studies

To study biodistribution in mice bearing LS174T xenografts, 16 mice were randomly divided in four groups with four animals each. One group of mice was s.c. injected with 555 μg of unlabelled recombinant $Z_{HER2:342}$ in 250 μl PBS 1 h before the injection of radioactivity. All mice were s.c. injected with 1 μg ^{99m}Tc-MAG3-$Z_{HER2:342}$ in 100 μl PBS (~100 kBq). At 2, 4 and 6 h p.i., one group of mice was intraperitoneally injected with a lethal dose of ketamine HCl (Ketalar, Pfizer) and xylazine HCl (Rompun, Bayer). The mice were killed with heart puncture with a 1-ml syringe rinsed with diluted heparin (Leo Pharma). The mice in the blocking group were killed 4 h p.i. Organs and tissue samples of blood, colon, heart, salivary glands, lung, thyroid, liver, tumour, spleen, muscle, pancreas, bone, kidney, brain, and stomach were excised and collected in weighed plastic bottles. Colon and stomach were cleaned from content in this experiment. Blood and tumour samples were taken from animals in the blocked group.

Organs and tissue samples were weighed and their radioactivity was recorded using an automatic gamma spectrometer with standard ^{99m}Tc protocol. The background was measured for each sample holder in the same way. Tissue uptake values were calculated as percent of injected activity per gram tissue (% IA/g).

To quantify hepatobiliary excretion, a group of three non-tumour-bearing Balb/c *nu*/*nu* mice were injected with ~1 μg ^{99m}Tc-MAG3-$Z_{HER2:342}$ (~100 kBq). The biodistribution measurement was performed 4 h p.i. according to the protocol described above, but intestines were collected together with their content and their radioactivity was measured.

For comparison, biodistribution of recombinant $Z_{HER2:342}$ indirectly labelled using *para*-iodobenzoate (^{125}I-PIB-$Z_{HER2:342}$) was performed 6 h p.i. in Balb/c *nu*/*nu* mice bearing LS174T xenografts. This conjugate was prepared according to Orlova et al. [35]. Approximately 30 kBq per animal was injected, and the mass of injected Affibody molecules was the same (about 1 μg per mouse) as in experiments with ^{99m}Tc-MAG3-$Z_{HER2:342}$.

An unpaired t test of the biodistribution data was performed employing the GraphPad Prism software (Graph-Pad Software Inc., San Diego, CA). Differences were considered significant if p values were less than 0.05.

Table 1 Biophysical characterisation data of $Z_{HER2:342}$ and MAG3-$Z_{HER2:342}$

Peptide	Synthetic yield (%)[a]	Theoretical molecular weight (Da)	Experimental molecular weight (Da) [b]	Dissociation constant (*M*) [c]	Melting point, (°C)[d]
$Z_{HER2:342}$	21	6,718	6,718	8×10^{-11}	64
MAG3-$Z_{HER2:342}$	16	7,021	7,020	20×10^{-11}	64

[a] Synthetic yields were calculated from RP-HPLC elution profiles
[b] Molecular weights were determined by ESI-MS
[c] The dissociation constants were determined by SPR biospecific interaction analysis
[d] Melting point analyses were performed by variable temperature circular dichroism

Imaging

Experimental tumour imaging was performed 6 h after injection in three mice bearing LS174T xenografts. All animals were intravenously injected (tail) with 3 MBq (3 μg) ^{99m}Tc-MAG3-$Z_{HER2:342}$. For imaging specificity control, HER2 receptors were pre-blocked in one mouse by subcutaneous injection of 0.5 mg recombinant non-radioactive $Z_{HER2:342}$ in PBS 1 h before injection of ^{99m}Tc-MAG3-$Z_{HER2:342}$. Six hours after injection of ^{99m}Tc-MAG3-$Z_{HER2:342}$, all animals were killed by over-dosing of ketamine/xylazine. Imaging was performed using a Siemens e.cam gamma camera equipped with an LEHR collimator at the Department of Nuclear Medicine of Uppsala University Hospital. Static images were collected over 10 min.

The imaging 24 h after injection was performed in one mouse bearing LS174T xenograft (low HER2 expression) and one mouse bearing SKOV-3 xenograft (high HER2 expression). The animals were injected with 20 MBq (3 μg) ^{99m}Tc-MAG3-$Z_{HER2:342}$. Imaging was performed according to the protocol described above, but the acquisition time was 30 min.

After imaging the mice from the non-blocked group were dissected. Organs and tissue samples of liver, kidney, caecum, caecum content, stomach, stomach content, large intestine, small intestine and muscle were excised and collected in weighed plastic bottles.

Organs and tissue samples were weighed and their radioactivity was recorded using an automatic gamma spectrometer with standard ^{99m}Tc protocol.

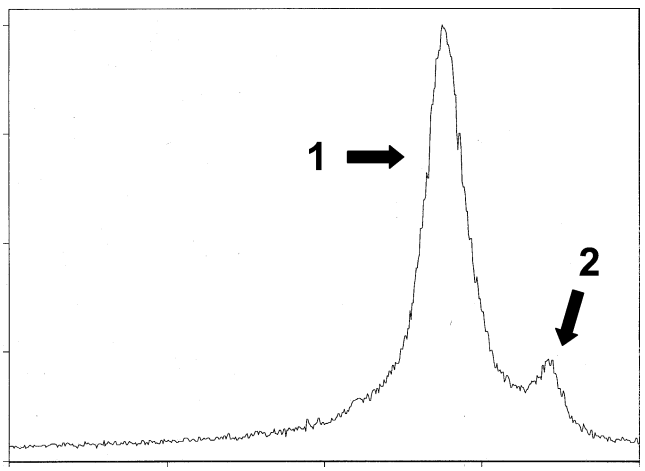

Fig. 1 Analysis of ^{99m}Tc-MAG3-$Z_{HER2:342}$ stability in serum. A sample was incubated in blood serum for 1 h at 37°C and analysed using SDS PAGE, and radioactivity distribution on gel was measured. *Peak 1* corresponds to the peak of ^{99m}Tc-MAG3-$Z_{HER2:342}$ stored in PBS; *peak 2* corresponds to ^{99m}Tc-pertechnetate

Results

Peptide synthesis

$Z_{HER2:342}$ was successfully synthesised using Fmoc solid phase peptide synthesis. The synthetic yield was determined to be 21% by analytical RP-HPLC. The Tc-chelating MAG3 moiety was introduced on the N-terminus by

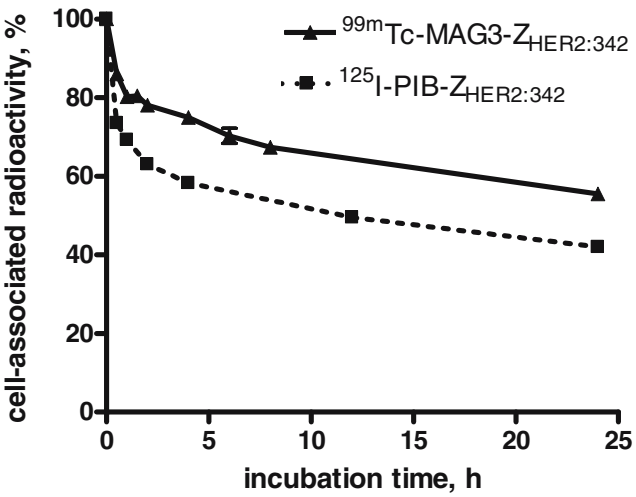

Fig. 2 Comparison of the cellular retention of ^{99m}Tc-MAG3-$Z_{HER2:342}$ (*triangles*), and ^{125}I-PIB-$Z_{HER2:342}$ (*squares*) in SKOV-3 cells. The cell-associated radioactivity at time zero after the interrupted incubation was normalised to unity. All data points are mean values of three measurements, and *error bars* present SEM (not seen in the majority of points because they are smaller than the symbols)

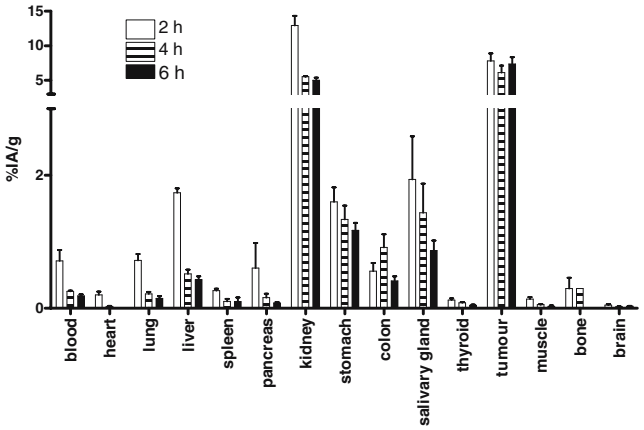

Fig. 3 Biodistribution of ^{99m}Tc-MAG3-$Z_{HER2:342}$ in Balb/c *nu*/*nu* mice with LS174T xenografts. Data are presented as % IA/g (average from four animals ±SEM). Data for thyroid are presented as % IA per organ

manual synthesis. The total yield of MAG3-$Z_{HER2.342}$ was 16%. The peptides were purified to more than 90% purity. The mass of each peptide was determined by electrospray ionisation mass spectrometry (ESI-MS), and the experimentally determined molecular weights correlated well with the theoretically calculated values (Table 1).

Biophysical analysis

Circular dichroism spectroscopy was used to analyse the peptide secondary structure. Both conjugates generated very similar characteristic α-helical spectra. Identical CD spectra were taken before and after a melting point test was performed, indicating that the peptides regained their original fold after melting. As indicated in Table 1, both conjugates have a melting point of 64°C.

Biosensor analysis

Biospecific interaction analysis was performed on a Biacore 2000 in order to study the effect of the MAG3 extension on the binding affinity. $Z_{HER2:342}$ had an apparent dissociation constant of 80 p*M*, whereas the corresponding value for MAG3-$Z_{HER2:342}$ proved to be somewhat higher, 200 p*M*, as shown in Table 1.

Radiolabelling

Labelling efficiency was 82±12% (n=15). The presence of reduced hydrolysed technetium was less than 2% in all experiments.

After labelling, ^{99m}Tc-MAG3-$Z_{HER2:342}$ was purified using size-exclusion chromatography with disposable NAP-5. In the radiopharmaceutical preparation kit, this column should be sterilised before use. The use of PBS as an eluent made it possible to obtain ^{99m}Tc-MAG3-$Z_{HER2:342}$ directly in an injectable form after purification. Losses of labelled conjugate during purification were in the order of 3–7%. According to the ITLC analysis of the purified product, its purity was always better that 98%. Labels were stable in PBS. After 1 h incubation with a 300-fold excess of cysteine at 37°C, 87.5±1.8% of the radioactivity was associated with the Affibody molecule.

SDS PAGE of ^{99m}Tc-MAG3-$Z_{HER2:342}$, which was incubated with blood serum at 37°C for 1 h, revealed two peaks of radioactivity along the lane (Fig. 1). A relatively short incubation time was selected because of quick clearance of conjugate from blood. The major peak (peak 1) corresponds to the peak of ^{99m}Tc-MAG3-$Z_{HER2:342}$, which was not exposed to blood serum, and contains more than 90% of radioactivity (better quantification is complicated owing to incomplete peak resolution). The smaller peak (peak 2) corresponds to ^{99m}Tc-pertechnetate. No other peaks were observed, indicating that stable transchelation of technetium to blood plasma proteins does not occur.

Cell binding and retention studies

To demonstrate that the binding was receptor specific, a large excess of unlabelled $Z_{HER2:342}$ was added to cells in the control experiments in order to saturate binding sites on HER2. The results of the binding specificity experiments showed that the binding of ^{99m}Tc-MAG3-$Z_{HER2:342}$ could be prevented by receptor saturation. Cell-bound radioactivity was reduced from 50.4±0.2% of added radioactivity to 1.5±0.02%. The antigen binding capacity for ^{99m}Tc-MAG3-$Z_{HER2:342}$ was 86±1%. It should be noted that the method used in this study for determination of antigen binding capacity underestimates antigen binding fraction in comparison with Lindmo analysis. However, it is a much less laborious method that is commonly used (see, e.g. [53]).

The radioactivity retention pattern after interrupted incubation with ^{99m}Tc-MAG3-$Z_{HER2:342}$ and ^{125}I-PIB-

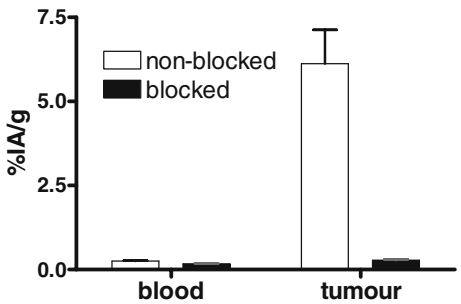

Fig. 4 Specificity of ^{99m}Tc-MAG3-$Z_{HER2:342}$ uptake in LS174T xenografts 4 h p.i. Data are presented as % IA/g (an average from four animals ±SEM). For receptor saturation, animals in blocking group were s.c. injected with 555 μg of unlabelled recombinant $Z_{HER2:342}$ 1 h before the injection of radioactivity

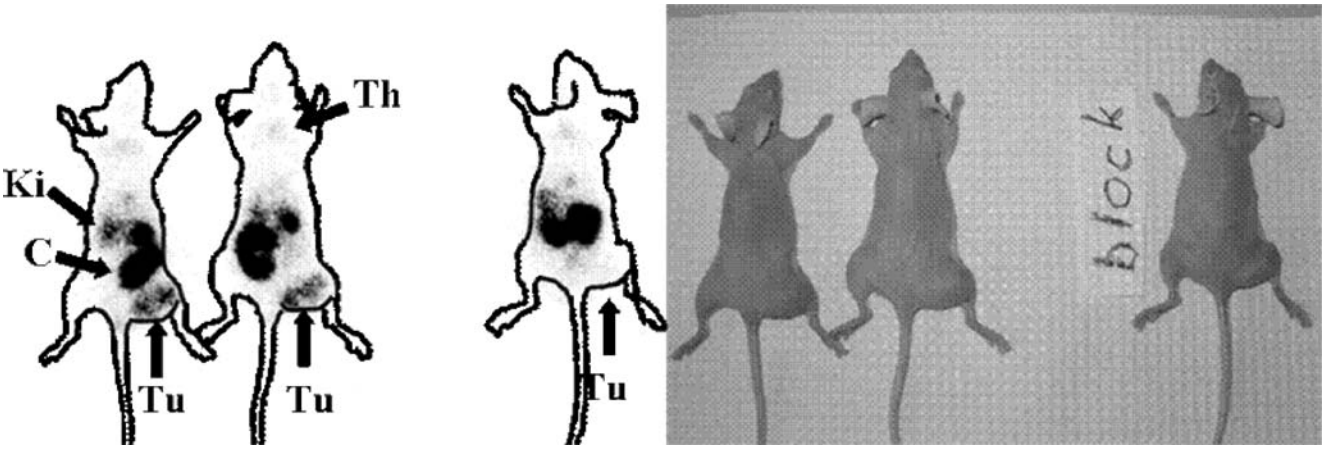

Fig. 5 An anterior gamma camera image 6 h p.i. (*left panel*) and photograph (*right panel*) of three Balb/c *nu*/*nu* mice bearing LS174T xenografts. HER2 receptors in the animal on the right were pre-saturated by injection of 500 μg of unlabelled recombinant $Z_{HER2:342}$ 45 min before injection of radiolabelled conjugate. *Tu* tumour, *Ki* kidney, *Th* thyroid, *C* caecum

$Z_{HER2:342}$ is shown in Fig. 2. Retention of the radioiodinated conjugate was reasonably good, with about 40% radioactivity still associated with cells 24 h after interrupted incubation. This might indicate that internalisation and intracellular degradation of $Z_{HER2:342}$ conjugates occur more slowly than internalisation and degradation of, for example, hEGF-based conjugates [52]. The cellular retention of ^{99m}Tc-MAG3-$Z_{HER2:342}$ was, however, better than the retention of ^{125}I-PIB-$Z_{HER2:342}$, resulting in 55% of cell-associated radioactivity 24 h after interrupted incubation.

Tumour targeting in Balb/c *nu*/*nu* mice with LS174T xenografts

Biodistribution data are presented in Fig. 3. The biodistribution was characterised by quick clearance of radioactivity from blood and all organs and tissues (the radioactivity of intestine content was not measured in this study). The radioactivity concentration in tumour xenograft was relatively high (about 7% IA/g) and constant during this experiment (no significant difference in tumour uptake at 2, 4 and 6 h p.i.). The radioactivity concentration in tumours was higher than in other organs or tissues except kidneys at 2 h p.i. Pre-injection of unlabelled $Z_{HER2.:342}$ decreased tumour uptake 4 h p.i. from 6.12±2.02 to 0.28±0.05% IA/g (p=0.001) (Fig. 4), indicating that the radioactivity uptake in tumours was HER2 specific. The combination of reasonably good retention of technetium in tumours and high blood and whole-body clearance generated good contrast with the majority of the organs and tissue. For example, tumour-to-blood ratios were 12.5, 23.8 and 39.3 at 2, 4 and 6 h p.i., respectively. The decrease in radioactivity in kidney was rather quick and the tumour-to-kidney ratio exceeded unity at 4 h p.i.

Table 2 Radioactivity concentration in samples taken after the imaging experiment

Organ	Radioactivity concentration (cpm/g) [a]
Liver	160,000±30,000
Kidney	1,708,000±205,000
Stomach[b]	311,000±65,000
Stomach content	1,202,000±630,000
Small intestine [b]	121,000±21,000
Caecum [b]	172,000±76,000
Caecum content	9,470,000±185,000
Large intestine [b]	134,000±46,000
Muscle	16,000±5,500

[a] Data are presented as counts per minute (cpm) per gram of sample
[b] Samples of stomach, caecum, and small and large intestines may have been contaminated to some extent with content of these organs

Imaging

Gamma camera imaging 6 h p.i. demonstrated clear accumulation of radioactivity in tumours (Fig. 5). This accumulation was receptor specific, since it could be blocked by pre-saturation of receptors with non-radioactive $Z_{HER2:342}$. The radioactivity accumulation in kidneys was approximately on the same level as in tumours. The radioactivity accumulation in thyroid was detected, which indicates that a certain release of ^{99m}Tc-pertechnetate in vivo occurred. However, the highest accumulation of radioactivity was detected in the abdominal region, in an area anatomically distinct from tumour, kidneys and liver, which resembled the caecum. In order to verify the exact localisation of the radioactivity, animals from the non-blocked group were dissected, and the radioactivity concentration in organs and gastro-intestinal tract content was measured (Table 2). These measurements demonstrated that the highest radioactivity was found in the caecum content and not in the

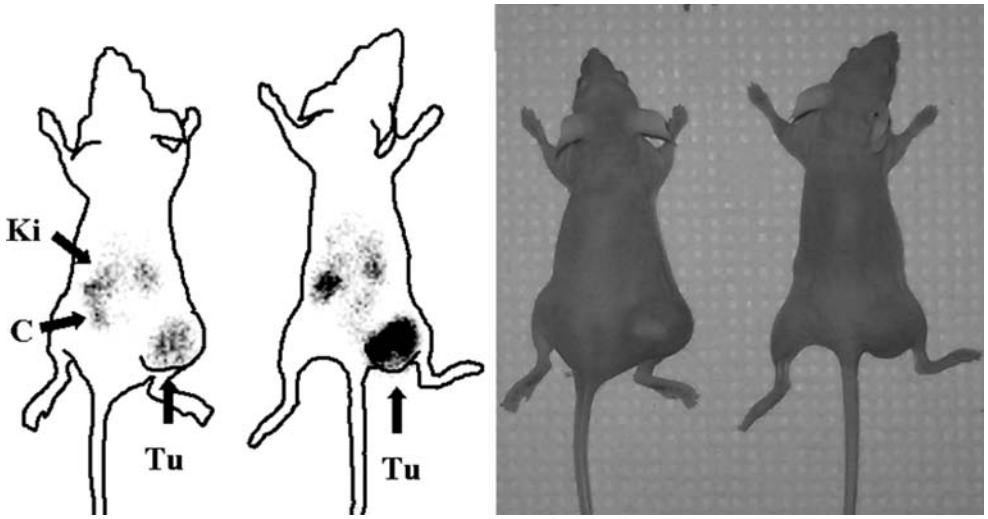

Fig. 6 An anterior gamma camera image obtained 24 h p.i. using ^{99m}Tc-MAG3-$Z_{HER2:342}$ (*left panel*) and photograph (*right panel*) of Balb/c *nu*/*nu* mice bearing LS174T (low HER2 expression) and SKOV-3 (high HER2 expression) xenografts. *Tu* tumour, *Ki* kidney, *C* caecum

wall of the caecum, indicating that hepatobiliary excretion is an essential pathway of conjugate excretion.

Imaging performed 24 h p.i. (Fig. 6) showed that radioactivity was almost completely cleared from the intestine, and mainly tumours and kidneys were visualised. The high HER2-expressing SKOV-3 xenograft accumulated more radioactivity than the low HER2-expressing LS174T xenograft.

Biodistribution in non-tumour-bearing Balb/c *nu*/*nu* mice

To verify that the hepatobiliary route plays an essential role in ^{99m}Tc-MAG3-$Z_{HER2:342}$ excretion, an additional biodistribution experiment in three non-tumour-bearing Balb/c *nu*/*nu* mice was performed 4 h p.i. In this experiment the radioactivity in whole intestines with content was measured (Table 3). The results showed low uptake in all organs and tissues, confirming the biodistribution data for tumour-bearing mice. It was found that about 30% of the injected radioactivity was collected in the intestines.

Comparison with biodistribution of ^{125}I-PIB-$Z_{HER2:342}$

Our earlier experiments in in vivo targeting of HER2 using radioiodinated, radiobrominated and indium-labelled $Z_{HER2:342}$ were performed using SKOV-3 xenografts, which express a high level of HER2 [33–36, 39]. The in vivo tumour models in this study were based on LS174T xenografts, which have low levels of HER2 expression. Therefore, direct comparison of tumour targeting properties of ^{99m}Tc-MAG3-$Z_{HER2:342}$ with properties of conjugates that have been characterised previously was not really correct. To make such a comparison possible, we performed a single time point (6 h p.i.) biodistribution study of ^{125}I-PIB-$Z_{HER2:342}$ in mice bearing LS174T xenografts. The comparison of the biodistribution of ^{99m}Tc-MAG3-$Z_{HER2:342}$ and ^{125}I-PIB-$Z_{HER2:342}$ is graphically presented in Fig. 7. According to this experiment, there was no significant difference between the conjugates in the radioactivity concentration in blood, spleen, salivary gland, tumour and muscle. The technetium accumulation was statistically significantly ($p<0.05$) lower than that of iodine in lung, liver, kidneys and thyroid. However, the technetium radioactivity in the stomach was higher than the radioactivity of radioiodine.

Discussion

We have previously demonstrated the feasibility of specific imaging of HER2 expression in xenograft models using the Affibody molecule $Z_{HER2:342}$ labelled with radioactive iodine, bromine or indium. Still, further development of Affibody molecule targeting is desirable, such as the use of

Table 3 Biodistribution of ^{99m}Tc-MAG3-$Z_{HER2:342}$ in non-tumour-bearing Balb/c *nu*/*nu* mice 4 h p.i.

Organ/tissue	Uptake(% IA/g)[a]
Blood	0.13±0.01
Lung	0.23±0.12
Liver	0.66±0.16
Spleen	0.06±0.01
Kidney	5.98±1.14
Stomach	0.15±0.04
Salivary gland	0.09±0.00
Skin	0.14±0.04
Muscle	0.02±0.00
Carcass [b]	3.36±0.60
Intestines with content [b]	29.84±10.83

[a] Data are presented as an average from three animals ±SEM
[b] Data for carcass and intestines (including caecum) with content are expressed as % IA per whole sample

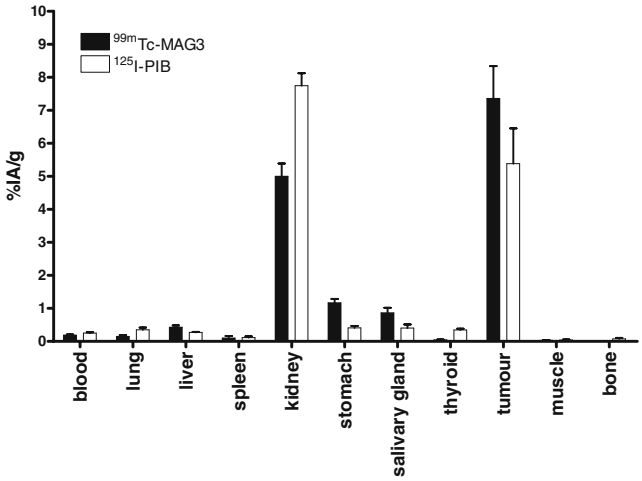

Fig. 7 Biodistribution comparison (6 h p.i.) of ^{99m}Tc-MAG3-$Z_{HER2:342}$ and ^{125}I-PIB- $Z_{HER2:342}$ in Balb/c *nu/nu* mice bearing LS174T xenografts. Data are presented as an average from four animals ±SEM. Data for the thyroid with content are presented as % IA per whole sample

^{99m}Tc, which would facilitate the introduction of Affibody molecule-mediated imaging into clinical practice owing to the excellent detection and dosimetric properties of this nuclide, as well as its excellent logistics.

The major advantage of using a small non-immunoglobulin-originating molecule such as the Affibody molecule as a targeting agent is, of course, the quick tumour localisation and quick clearance from non-specific compartments. Another advantage is that it can be produced by complete chemical synthesis. By choosing a synthetic production route rather than recombinant expression, the chelating moiety can be introduced site specifically and the modified peptide can be purified to homogeneity. In addition, the use of peptide synthesis instead of recombinant technology can reduce production costs by about one-half, and make the tracer more available. In this paper, we describe the incorporation of an amino acid-based ^{99m}Tc-chelating sequence into the parental $Z_{HER2:342}$ molecule by standard coupling chemistry.

The biophysical characterisation of the synthetic Affibody molecules showed a successful synthesis in a yield of 16–21%, which is considered good for peptides with a length of about 60 amino acids. Correct identities of both $Z_{HER2:342}$ and MAG3-$Z_{HER2:342}$ were confirmed with ESI-MS. The affinity of the synthetic peptide was 80 p*M*. Although the incorporation of MAG3 slightly reduced the affinity to 200 p*M*, it was still in the subnanomolar range, which is compatible with in vivo imaging [54].

MAG3-$Z_{HER2:342}$ was labelled with ^{99m}Tc with an average efficiency of about 80%, comparable to the reported values (40–60%) for S-acetyl protected pre-conjugated MAG3 to HNE2, which is of similar size [40], though somewhat lower than the reported yield (93–97%) for the smaller MAG3-RC-160 and MAG3-TOC [45]. The question of the necessity of protecting the thiol group in conjugated MAG3 is controversial (as discussed, for example, by Hnatowich and co-workers [55]). In this study, non-protected mercaptoacetyl was successfully used, even after 10 months' storage in the freezer. In vitro experiments demonstrated that the radiolabelled Affibody molecules retained the capacity to bind specifically to HER2-expressing SKOV-3 cells. In vitro cellular retention of radioactivity delivered by ^{99m}Tc-MAG3-$Z_{HER2:342}$ was better than that of radioactivity delivered by radiohalogenated $Z_{HER2:342}$.

The biodistribution studies indicated an adequate in vivo stability of the ^{99m}Tc-MAG3 label on $Z_{HER2:342}$. The blood clearance was quick, indicating that there was no transchelation of ^{99m}Tc to blood plasma proteins. This finding is in agreement with serum stability study. The low uptake in liver, spleen and lung excluded the formation of colloids of any size in the course of label catabolism. Still, ^{99m}Tc radioactivity accumulation in the stomach was significantly higher than for radioiodine, and comparison with ^{111}In-benzyl-DPTA-$Z_{HER2:342}$ [39] shows higher accumulation of ^{99m}Tc in the stomach, salivary gland and thyroid. Since these organs are known to accumulate pertechnetate, we cannot exclude the possibility that some release of free pertechnetate occurred. Note that some release of pertechnetate was found in the serum stability test in vitro.

The biodistribution and imaging studies showed that ^{99m}Tc-MAG3-$Z_{HER2:342}$ can target HER2-expressing xenografts, even when a cell line with low HER2 expression (LS174T) is used. The targeting is highly receptor specific and provides a favourable tumour-to-non-tumour ratio owing to quick tumour localisation and clearance from blood and non-specific organs. Assuming that this biodistribution pattern could be translated into humans, imaging of HER2 expression in primary breast tumours and liver, lung, brain and a majority of bone metastases should be possible using ^{99m}Tc-MAG3-$Z_{HER2:342}$. In this animal model, the use of the ^{99m}Tc label provided a similar or better tumour-to-organ ratio for all studied organs in comparison with use of the much more expensive radioiodine.

The hepatobiliary excretion of ^{99m}Tc-MAG3-$Z_{HER2:342}$ might necessitate imaging on the day after injection to detect HER2 expression in extrahepatic metastases in the abdominal area and ovarian carcinoma. The results of this study show that high-contrast images can be obtained 24 h after injection. The feasibility of such an approach has been demonstrated in the clinics with ^{99m}Tc-labelled antibody fragments [56, 57]. Imaging on the day of injection would have apparent advantages. For this reason, we consider further development of the concept of synthetic Affibody molecules with an incorporated ^{99m}Tc-chelating moiety to be desirable.

The biodistribution and imaging study results indicate that ^{99m}Tc-MAG3-$Z_{HER2:342}$ can be used for detection of

HER2 expression in malignant tumours and in myocardium of cancer patients. This might make it possible to select patients for Herceptin treatment, and to identify patients at risk of cardiotoxicity due to such therapy.

Acknowledgements This study was financially supported by Affibody AB and grants from the Swedish Cancer Society and Swedish Research Council (VR). We thank Veronika Eriksson at BMS and the animal facility staff of Rudbeck laboratory for technical assistance, and Gustav Sundqvist at KTH for running the ESI-MS analyses. We thank Dr. Joachim Feldwisch, Dr. Anders Wennborg and Dr. Lars Abrahmsén (Affibody AB) for interesting and inspiring discussions on the use of Affibody molecules for imaging and for comments on the manuscript.

References

1. Aunoble B, Sanches R, Didier E, Bignon YJ. Major oncogenes and tumor suppressor genes involved in epithelial ovarian cancer. Int J Oncol 2000;16:567–76.
2. Carlsson J, Nordgren H, Sjostrom J, Wester K, Villman K, Bengtsson NO, et al. HER2 expression in breast cancer primary tumours and corresponding metastases. Original data and literature review. Br J Cancer 2004;90:2344–8.
3. Gardmark T, Wester K, de la Torre M, Carlsson J, Malmstrom PU. Analysis of HER2 expression in primary urinary bladder carcinoma and corresponding metastases. BJU Int 2005;95: 982–6.
4. Muss HB, Thor AD, Berry DA, Kute T, Liu ET, Koerner F, et al. c-erbB-2 expression and response to adjuvant therapy in women with node-positive early breast cancer. N Engl J Med 1994; 330:1260–6.
5. Paik S, Bryant J, Park C, Fisher B, Tan-Chiu E, Hyams D, et al. erbB-2 and response to doxorubicin in patients with axillary lymph node-positive, hormone receptor-negative breast cancer. J Natl Cancer Inst 1998;90:1361–70.
6. Allred DC, Clark GM, Elledge R, Fugua SA, Brown RW, Chamness GC, et al. Association of p53 protein expression with tumor cell proliferation rate and clinical outcome in node-negative breast cancer. J Natl Cancer Inst 1993;85:200–6.
7. Gusterson BA, Gelber RD, Goldhirsch A, Price KN, Save-Soderborgh J, Anbazhagan R, et al. Prognostic importance of c-erbB-2 expression in breast cancer. J Clin Oncol 1992;10:1049–56.
8. Giai M, Roagna R, Ponzone R, De Bortoli M, Dati C, Sismondi P. Prognostic and predictive relevance of c-erbB-2 and ras expression in node positive and negative breast cancer. Anticancer Res 1994;14:1441–50.
9. Tetu B, Brisson J. Prognostic significance of HER-2/neu oncoprotein expression in node-positive breast cancer: The influence of the pattern of immunostaining and adjuvant therapy. Cancer 1994;73:2359–65.
10. Bast RC Jr, Ravdin P, Hayes DF, Bates S, Fritsche H Jr, Jessup JM, et al. American Society of Clinical Oncology Tumor Markers Expert Panel. 2000 update of recommendations for the use of tumor markers in breast and colorectal cancer: clinical practice guidelines of the American Society of Clinical Oncology. J Clin Oncol 2001;19:1865–78.
11. Behr TM, Behe M, Wormann B. Trastuzumab and breast cancer. N Engl J Med 2001;345:995–6.
12. De Santes K, Slamon D, Anderson SK, Shepard M, Fendly B, Maneval D, et al. Radiolabeled antibody targeting of the HER-2/neu oncoprotein. Cancer Res 1992;52:1916–23.
13. Xu FJ, Yu YH, Bae DS, Zhao XG, Slade SK, Boyer CM, et al. Radioiodinated antibody targeting of the HER-2/neu oncoprotein. Nucl Med Biol 1997;24:451–9.
14. Zalutsky MR, Xu FJ, Yu Y, Foulon CF, Zhao XG, Slade SK, et al. Radioiodinated antibody targeting of the HER-2/neu oncoprotein: effects of labeling method on cellular processing and tissue distribution. Nucl Med Biol 1999;26:781–90.
15. Tsai SW, Sun Y, Williams LE, Raubitschek AA, Wu AM, Shively JE. Biodistribution and radioimmunotherapy of human breast cancer xenografts with radiometal-labeled DOTA conjugated anti-HER2/neu antibody 4D5. Bioconjug Chem 2000; 11:327–34.
16. Garmestani K, Milenic DE, Plascjak PS, Brechbiel MW. A new and convenient method for purification of ^{86}Y using a Sr(II) selective resin and comparison of biodistribution of ^{86}Y and ^{111}In labeled Herceptin. Nucl Med Biol 2002;29:599–606.
17. Lub-de Hooge MN, Kosterink JG, Perik PJ, Nijnuis H, Tran L, Bart J, et al. Preclinical characterisation of ^{111}In-DTPA-trastuzumab. Br J Pharmacol 2004;143:99–106.
18. Persson M, Gedda L, Jensen HJ, Lundqvist H, Malmström P-U, Tolmachev V. Astatinated trastuzumab, a putative agent for radionuclide immunotherapy of ErbB2 expressing tumors. Oncol Rep 2006;15:673–80.
19. Persson M, Tolmachev V, Andersson K, Gedda L, Sandström M, Carlsson J. [^{177}Lu]pertuzumab. Experimental studies on targeting of HER-2 positive tumour cells. Eur J Nucl Med Mol Imaging 2005;32:1457–62.
20. Batra SK, Jain M, Wittel UA, Chauhan SC, Colcher D. Pharmacokinetics and biodistribution of genetically engineered antibodies. Curr Opin Biotechnol 2002;13:603–8.
21. Britz-Cunningham SH, Adelstein J. Molecular targeting with radionuclides: state of the science. J Nucl Med 2003;44:1945–61.
22. Adams GP, McCartney JE, Tai MS, Oppermann H, Huston JS, Stafford WF 3rd, et al. Highly specific in vivo tumor targeting by monovalent and divalent forms of 741F8 anti-c-erbB-2 single-chain Fv. Cancer Res 1993;53:4026–34.
23. Olafsen T, Tan GJ, Cheung CW, Yazaki PJ, Park JM, Shively JE, et al. Characterization of engineered anti-p185HER-2 (scFv-CH3) 2 antibody fragments (minibodies) for tumor targeting. Protein Eng Des Sel 2004;17:315–23.
24. Smith-Jones PM, Solit DB, Akhurst T, Afroze F, Rosen N, Larson SM. Imaging the pharmacodynamics of HER2 degradation in response to Hsp90 inhibitors. Nat Biotechnol 2004;22:701–6.
25. Tang Y, Wang J, Scollard DA, Mondal H, Holloway C, Kahn HJ, et al. Imaging of HER2/neu-positive BT-474 human breast cancer xenografts in athymic mice using ^{111}In-trastusumab (Herceptin) Fab fragments. Nucl Med Biol 2005;32:51–8.
26. Nord K, Gunneriusson E, Ringdahl J, Ståhl S, Uhlén M, Nygren PÅ. Binding proteins selected from combinatorial libraries of an alpha-helical bacterial receptor domain. Nat Biotechnol 1997;15:772–7.
27. Nord K, Gunneriusson E, Uhlén M, Nygren PÅ. Ligands selected from combinatorial libraries of protein A for use in affinity capture of apolipoprotein A-1M and taq DNA polymerase. J Biotechnol 2000;80:45–54.
28. Rönnmark J, Hansson M, Nguyen T, Uhlén M, Robert A, Ståhl S, et al. Construction and characterization of affibody-Fc chimeras produced in *Escherichia coli*. J Immunol Methods 2002;261:199–211.
29. Rönnmark J, Kampf C, Asplund A, Höiden-Guthenberg I, Wester K, Ponten F, et al. Affibody-beta-galactosidase immunoconjugates produced as soluble fusion proteins in the *Escherichia coli* cytosol. J Immunol Methods 2003;281:149–60.
30. Renberg B, Shiroyama I, Engfeldt T, Nygren PK, Karlström AE Affibody protein capture microarrays: synthesis and evaluation of random and directed immobilization of affibody molecules. Anal Biochem 2005;341:334–43.

31. Wikman M, Steffen AC, Gunneriusson E, Tolmachev V, Adams GP, Carlsson J, et al. Selection and characterisation of HER2/neu-binding affibody ligands. Protein Eng Des Sel 2004;17:455–62.
32. Steffen AC, Wikman M, Tolmachev V, Adams GP, Nilsson F, Ståhl S, et al. In vitro characterization of a bivalent anti-HER-2 affibody with potential for radionuclide based diagnostics. Cancer Biother Radiopharm 2005;20:239–48.
33. Steffen AC, Orlova A, Wikman M, Nilsson FY, Stahl S, Adams GP, et al. Affibody mediated tumor targeting of HER-2 expressing xenografts in mice. Eur J Nucl Med Mol Imaging 2006;33:631–8.
34. Mume E, Orlova A, Nilsson F, Larsson B, Nilsson AS, Sjöberg S, et al. Evaluation of (4-hydroxyphenyl)ethyl)maleimide for site-specific radiobromination of anti-HER2 affibody. Bioconjugate Chem 2005;16:1547–55.
35. Orlova A, Magnusson M, Eriksson T, Nilsson M, Larsson B, Höiden-Guthenberg I, et al. Tumor imaging using a picomolar affinity HER2 binding affibody molecule. Cancer Res 2006;66:4339–48.
36. Tolmachev V, Nilsson FY, Widström C, Andersson K, Gedda L, Wennborg A, et al. ^{111}In-benzyl-DTPA-$Z_{HER2:342}$, an Affibody-based conjugate for in vivo imaging of HER2 expression in malignant tumors. J Nucl Med 2006;47:846–53.
37. Orlova A, Nilsson F, Magnusson M, Gedda L, Widstrom C, Wennborg A, et al. ^{111}In-Bz-DTPA-ZHER2:342, a candidate for imaging of HER2-expression in malignant tumors. J Lab Comp Radiopharm 2005;48 Suppl 1:S51.
38. Liu S, Edwards DS. ^{99m}Tc-labeled small peptides as diagnostic radiopharmaceuticals. Chem Rev 1999;99:2235–68.
39. Orlova A, Nilsson F, Wikman M, Ståhl S, Carlsson J, Tolmachev V. Comparative in vivo evaluation of iodine and technetium labels on anti-HER2 affibody for single-photon imaging of HER2 expression in tumors. J Nucl Med 2006;47:512–9.
40. Zhu Z, Wang Y, Zhang Y, Liu G, Liu N, Rusckowski M, et al. A novel and simplified route to the synthesis of N3S chelators for ^{99m}Tc labeling. Nucl Med Biol 2001;28:703–8.
41. Qu T, Wang Y, Zhu Z, Rusckowski M, Hnatowich DJ. Different chelators and different peptides together influence the in vitro and mouse in vivo properties of ^{99}Tc^{m}. Nucl Med Commun 2001;22:203–15.
42. Lei K, Rusckowski M, Chang F, Qu T, Mardirossian G, Hnatowich DJ. Technetium-99m antibodies labeled with MAG3 and SHNH: an in vitro and animal in vivo comparison. Nucl Med Biol 1996;23:917–22.
43. Kim MK, Jeong HJ, Kao CH, Yao Z, Paik DS, Pie JE, et al. Improved renal clearance and tumor targeting of ^{99m}Tc-labeled anti-Tac monoclonal antibody Fab by chemical modifications. Nucl Med Biol 2002;29:139–46.
44. Kobayashi H, Yoo TM, Kim IS, Kim MK, Le N, Webber KO, et al. L-Lysine effectively blocks renal uptake of I-125 or Tc-99m labeled anti-Tac disulfide-stabilized Fv fragment. Cancer Res 1996;56:3788–95.
45. Decristoforo C, Mather SJ. Preparation, ^{99m}Tc-labeling, and in vitro characterization of HYNIC and N_3S modified RC-160 and [Tyr3]octreotide. Bioconjugate Chem 1999;10:431–8.
46. Zhang YM, Liu N, Zhu ZH, Rusckowski M, Hnatowich DJ. Influence of different chelators (HYNIC, MAG3 and DTPA) on tumor cell accumulation and mouse biodistribution of technetium-99m labeled to antisense DNA. Eur J Nucl Med 2000;27:1700–7.
47. Engfeldt T, Renberg B, Brumer H, Nygren PÅ, Karlström AE. Chemical synthesis of triple-labelled three-helix bundle binding proteins for specific fluorescent detection of unlabelled protein. Chembiochem 2005;6:1043–50.
48. Blok D, Feitsma HI, Kooy YM, Welling MM, Ossendorp F, Vermeij P, et al. New chelation strategy allows for quick and clean ^{99m}Tc-labeling of synthetic peptides. Nucl Med Biol 2004;31:815–20.
49. Winnard P Jr, Chang F, Rusckowski M, Mardirossian G, Hnatowich DJ. Preparation and use of NHS-MAG3 for technetium-99m labeling of DNA. Nucl Med Biol 1997;24:425–32.
50. Milenic DE, Garmestani K, Brady ED, Albert PS, Ma D, Abdulla A, et al. Targeting of HER2 antigen for the treatment of disseminated peritoneal disease. Clin Cancer Res 2004;10:7834–41.
51. Milenic DE, Garmestani K, Brady ED, Albert PS, Ma D, Abdulla A, et al. α-Particle radioimmunotherapy of disseminated peritoneal disease using a ^{212}Pb-labeled radioimmunoconjugate targeting HER2. Cancer Biother Radiopharm 2005;20:557–68.
52. Orlova A, Bruskin A, Sjöström A, Lundqvist H, Gedda L, Tolmachev V. Cellular processing of ^{125}I and ^{111}In labeled epidermal growth factor (EGF) bound to cultured A431 tumor cells. Nucl Med Biol 2000;27:827–35.
53. Adams GP, Shaller CC, Dadachova E, Simmons HH, Horak EM, Tesfaye A, et al. A single treatment of yttrium-90-labeled CHX-A″-C6.5 diabody inhibits the growth of established human tumor xenografts in immunodeficient mice. Cancer Res 2004;64:6200–6.
54. Behr TM, Gotthardt M, Barth A, Behe M. Imaging tumors with peptide-based radioligands. Q J Nucl Med 2001;45:189–200.
55. Hnatowich DJ, Chang F, Lei K, Ruscowski M. The influence of temperature and alkaline pH on the labeling of free and conjugated MAG3 with technetium-99m. Appl Radiat lsot 1997;48:587–94.
56. Wegener WA, Petrelli N, Serafini A, Goldenberg DM. Safety and efficacy of arcitumomab imaging in colorectal cancer after repeated administration. J Nucl Med 2000;41:1016–20.
57. Fuster D, Maurel J, Muxi A, Setoain X, Ayuso C, Martin F, et al. Is there a role for ^{99m}Tc-anti-CEA monoclonal antibody imaging in the diagnosis of recurrent colorectal carcinoma? Q J Nucl Med 2003;47:109–15.